

Assessment of regional grey matter loss in dementia with Lewy bodies: a surface based MRI analysis.

Rosie Watson^{1,2} Sean J. Colloby¹ Andrew M. Blamire³ John T. O'Brien^{1,4}

¹Institute for Ageing and Health, Newcastle University, Campus for Ageing and Vitality, NE4 5PL, UK.

²Department of Aged Care, The Royal Melbourne Hospital, Parkville, Australia.

³Institute of Cellular Medicine & Newcastle Magnetic Resonance Centre, Newcastle University, Newcastle upon Tyne, UK

⁴Department of Psychiatry, University of Cambridge, Cambridge, UK

Authors

Rosie Watson PhD (Corresponding Author)

The Royal Melbourne Hospital – Royal Park Campus, Parkville, Victoria 3052, Australia

telephone: +61 3 8387 2000

fax: +61 3 8387 2222

email: rosie.watson@mh.org.au

Sean J. Colloby PhD

Andrew M. Blamire PhD

John T. O'Brien DM

Conflicts of interest and Source of Funding: Dr Watson, Dr Colloby and Professor Blamire report no disclosures. Professor O'Brien has been a consultant for GE Healthcare, Lilly, Bayer Healthcare, TauRx and Nutricia and has received honoraria for talks from GE Healthcare, Lilly and Novartis.

The study was funded by the Sir Jules Thorn Charitable Trust [grant ref: 05/JTA] and supported by the National Institute for Health Research (NIHR) Newcastle Biomedical Research Centre in Ageing and Chronic Disease and Biomedical Research Unit in Lewy Body Dementia based at Newcastle upon Tyne Hospitals NHS Foundation Trust and Newcastle University, and the Biomedical Research Centre and Unit in Dementia based at Cambridge University Hospitals NHS Foundation Trust. The views expressed are those of the author(s) and not necessarily those of the NHS, NIHR or the Department of Health.

Acknowledgements

We thank Dr Robert Barber for providing assistance with subject diagnostic rating as well as Josh Wood, Assistant Psychologist and members of NE-DeNDRoN, Karen Morgan and Barbara Wilson for their assistance with recruitment and assessment of study participants. We are also grateful to all of the study volunteers for their involvement.

Keywords: Dementia, Lewy body disease, Alzheimer's disease, MRI, neuroimaging

Word Count: 2933 (main text) + 214 (abstract)

Tables: 3

Figures: 2

References: 30

Abstract

Objective: To compare MRI patterns of cortical thinning in subjects with dementia with Lewy bodies (DLB), Alzheimer's disease (AD) and normal ageing and investigate the relationship between cortical thickness and clinical measures.

Methods: Study participants (31 DLB, 30 AD and 33 healthy comparison subjects) underwent 3 Tesla T₁-weighted MRI and completed clinical and cognitive assessments. We used the FreeSurfer analysis package to measure cortical thickness and investigated the patterns of cortical thinning across groups.

Results: Cortical thinning in AD was found predominantly in the temporal and parietal areas extending into the frontal lobes (n=63, df=59, t>3.3, p<0.005, FDR corrected). In DLB, cortical thinning was less diffuse with focal areas of cortical change predominantly affecting posterior structures (inferior parietal, posterior cingulate and fusiform gyrus) (n=64, df=60, t>3.6, p<0.005, FDR corrected). The average reduction in cortical thickness in medial temporal lobe structures was less in DLB (6-10%) than in AD (15-24%), and similar to the reduction in cortical thickness observed in other regions including inferior parietal, precuneus and posterior cingulate (6-9%). Associations between cortical thickness and clinical measures (MMSE and verbal fluency) were also observed in DLB (n=31, df=27, t>2.8, p<0.01 uncorrected).

Conclusion: Cortical thickness may be a sensitive measure for characterising grey matter loss in DLB and highlights important structural imaging differences between the conditions.

INTRODUCTION

Dementia with Lewy bodies and Alzheimer's disease (AD) are common forms of dementia yet the clinical separation between the conditions remains challenging. *In vivo* biomarkers are therefore required which can help differentiate between the conditions and improve our understanding of the clinical features observed. DLB and AD show some differences in regional structural atrophy on MRI with greater medial temporal lobe atrophy in AD. However, there are relatively few cortical differences observed despite marked differences seen with functional imaging.

Imaging techniques and analysis methods are becoming increasingly sensitive thereby improving their potential as a diagnostic technique. Measurement of cortical thickness (CTh) is an advanced method of structural image analysis. It allows the regional distribution and quantification of cortical loss to be specifically examined which is in contrast to gyral or lobar volumetric studies which often combine grey matter and white matter within regional volumes. Voxel based morphometry (VBM) does allow separate grey matter assessment, although results have been shown to be more closely related to alterations in cortical surface area and folding (1, 2). Studies have investigated CTh in AD (3, 4) however, regional patterns of CTh have not yet been assessed in DLB.

We aimed to investigate CTh in subjects with DLB compared to AD and similar aged healthy comparison subjects. We hypothesised that in AD, the pattern of cortical thinning would involve predominantly the temporal lobe, parietal association cortices and frontal regions. In contrast, the pattern of cortical thinning in DLB would be much less diffuse involving predominantly the posterior cortical structures. In an exploratory analysis, we investigated the association between CTh and clinical measures including MMSE, letter

fluency, visual hallucinations and UPDRS III. We hypothesised that areas of cortical thinning would be associated with poorer task performance and the tests would correlate with anatomical areas known to be necessary for their performance.

METHODS

Subjects, assessments and diagnosis

Seventy-one individuals over the age of 60 (36 subjects with probable AD (5) and 35 with probable DLB (6)) were recruited from a community dwelling population of patients referred to local Old Age Psychiatry, Geriatric Medicine or Neurology Services. All subjects underwent clinical and neuropsychological evaluations as previously described.(7) Thirty-five similar aged healthy subjects were recruited from among relatives and friends of subjects with dementia or volunteered via advertisements in local community newsletters.

The research was approved by the local ethics committee. All subjects or, where appropriate, their nearest relative, provided written informed consent.

Assessment of global cognitive measures in all subjects (AD, DLB and healthy subjects) included the Cambridge Cognitive Examination (CAMCOG) which incorporates the Mini-Mental State Examination (MMSE).(8) Motor parkinsonism was assessed with the Unified Parkinson's Disease Rating Scale Part III (UPDRS-III).(9) For subjects with dementia, neuropsychiatric features were assessed using the Neuropsychiatric Inventory (NPI)(10) and function was assessed using the Bristol Activities of Daily Living.(11)

MRI data acquisition

Subjects underwent T1 weighted MR scanning on a 3T MRI system using an 8 channel head coil (Intera Achieva scanner, Philips Medical Systems, Eindhoven, Netherlands) within 2 months of the study assessment, as previously described.(7) The sequence was a standard T1 weighted volumetric sequence covering the whole brain (3D MPRAGE, sagittal acquisition, 1 mm isotropic resolution and matrix size of 240 (anterior-posterior) x 240 (superior-inferior) x 180 (right-left); repetition time (TR) = 9.6ms; echo time (TE) = 4.6ms; flip angle = 8° ; SENSE factor = 2). The acquired volume was angulated such that the axial slice orientation was standardised to align with the AC-PC line.

Imaging processing

Estimates of CTh were performed from cortical surface reconstructions computed from T1w images using FreeSurfer (v. 4.5, <http://surfer.nmr.mgh.harvard.edu/>). The technical aspects of these methods have been described elsewhere.(12-14) In brief, the processing stream involves intensity non-uniformity correction, Talairach registration, removal of non-brain tissue (skull stripping), white matter (WM) and subcortical grey matter (GM) segmentation, tessellation of the GM-WM boundary then surface deformation following GM-CSF intensity gradients to optimally place GM-WM and GM-CSF borders.(12, 13) Once cortical models were generated, surface inflation, transformation to a spherical atlas and parcellation of the cerebral cortex into regions based on gyral and sulcal structure were carried out.(15) This technique used both intensity and continuity information from the entire 3D MR volume in the segmentation and deformation procedures to produce representations of CTh, calculated as the closest distance from the GM-WM to GM-CSF

boundaries at each vertex on the tessellated surface.(16) CTh measures were mapped to the inflated surface. All images were then aligned to a common surface template and smoothed with a 20mm full width at half maximum (FWHM) surface based Gaussian kernel.

Visual inspection of images at each step of the FreeSurfer processing stream was carefully carried out to ensure accurate Talairach transformations, skull strips, deep GM and white/pial surface generation and tissue classifications. During this procedure, skull strips and pial/WM surface errors were identified in 27 scans (6 healthy subjects, 13 AD, 8 DLB). In these subjects, a different skull stripping algorithm was applied using a brain masking approach prior to reapplication of the FreeSurfer processing stream (less skull stripping). This involved segmentation of the MR scan into GM, WM and cerebrospinal fluid (CSF) using the standard unified segmentation model in SPM8 (<http://www.fil.ion.ucl.ac.uk/spm>).(17) The segmented images were combined and thresholded to create individual brain mask images that were then applied to the original T1w scan, producing the skull stripped image. Modification to the processing stream resulted in successful cortical surface generation in 15 scans (4 healthy subjects, 7 AD, 4 DLB). However, the remaining 12 scans (2 healthy subjects, 6 AD, 4 DLB), still exhibited significant pial/WM surface errors and were therefore excluded (5F, 7M; mean age 80.2 (5.62); MMSE (AD, DLB) = 19.0 (4.34)). The dataset for subsequent CTh analysis comprised of 33 comparison subjects, 30 AD and 31 DLB.

Statistical analysis

The Statistical Package for Social Sciences software (SPSS ver. 19.0.0.1, <http://www-01.ibm.com/software/analytics/spss/>) was used for further statistical evaluation as required. Continuous variables were tested for normality using the Shapiro-Wilk test and visual inspection of histograms. Where appropriate, differences in demographic and clinical data were assessed using parametric (ANOVA, t-tests) and non-parametric tests (Kruskall-Wallis H, Mann-Whitney U). For categorical measures, χ^2 tests were applied. For each test statistic, a probability value of <0.05 was regarded as significant.

Cortical thickness

Regional CTh between groups were examined on a vertex-wise basis using the general linear model (GLM), performed with the QDEC software (<http://surfer.nmr.mgh.harvard.edu/fswiki/Qdec>). CTh was modelled as a function of group, controlling for effects of age and gender as nuisance covariates. $CTh = \beta_1 \text{ Group1} + \beta_2 \text{ Group2} + \beta_3 \text{ Age} + \beta_4 \text{ Gender} + \mu + \varepsilon$ (where μ is a constant and ε is error). Contrasts of interest were calculated using two-tailed t-tests between the group estimates β_1 and β_2 which represent either DLB vs. healthy older subjects, AD vs. healthy older subjects or DLB vs. AD. Surface maps showing significant differences between groups were generated. Effects of CTh on clinical variables (MMSE, letter fluency, visual hallucinations and UPDRS III) were also investigated in DLB and AD. CTh was modelled as a function of covariate of interest, controlling for effects of age and gender as nuisance covariates. $CTh = \beta_1 \text{ Behavioural variable} + \beta_2 \text{ Age} + \beta_3 \text{ Gender} + \mu + \varepsilon$. Contrasts of interest were calculated from the estimate β_1 , and whether β_1 was

significantly different from zero. Similarly, surface maps were created demonstrating significant behavioural correlates on CTh. For all statistical analyses, surface maps were presented as either corrected (false discovery rate approach (FDR) (18)) or uncorrected probabilities.

As well as surface maps, FreeSurfer also generated thickness measures from 33 cortical regions of interest for each hemisphere as described by Desikan *et al.*(15)

RESULTS

Subject characteristics

The demographic data for patients and healthy subjects are summarised in Table 1.

Subject groups were well matched for age and, for the AD and DLB groups mean CAMCOG and MMSE scores were similar. There were more men in the DLB group and as expected, the DLB group had significantly higher UPDRS III scores than the AD and healthy comparison group.

Comparison of AD and healthy subjects

The areas of cortical thinning in AD compared to healthy older individuals are represented in Figure 1 (a), (n=63, df=59, $t > 3.3$, $p < 0.005$, FDR corrected) and Table 2 (b). In AD, cortical thinning was diffuse and involved the temporal, parietal and frontal lobes. The most significant areas affected were, the entorhinal cortex and parahippocampal gyrus with an average reduction of 23-24% and 15-16% respectively when compared to healthy subjects (Table 3).

Comparison of DLB and healthy subjects

The areas of cortical thinning in DLB compared to healthy subjects are represented in Figure 1 (b), ($n=64$, $df=60$, $t>3.6$, $p<0.005$, FDR corrected) and Table 2 (a). In DLB, there was generally less cortical thinning than observed in AD compared to healthy subjects. There was a large cluster in the left inferior parietal area and smaller clusters in the left superior temporal and the left anterior and posterior cingulate. There were large clusters of significant cortical thinning observed in the right fusiform and right superior temporal gyri. Smaller clusters were found in the inferior parietal and superior temporal gyri and the right posterior cingulate.

Comparison of AD and DLB

When comparing AD and DLB, areas of significant thinning ($n=61$, $df=57$, $t>4.1$, $p<0.05$, FDR corrected) were located in the left medial temporal lobe structures – entorhinal cortex and parahippocampal gyri.

Cortical thickness in AD and DLB using the Desikan parcellation map

The average CTh reduction in AD and DLB compared to healthy older individuals using FreeSurfer Desikan parcellation regions of interest were also reviewed. Results for selected regions are represented in Table 3. In AD, reduction in CTh was diffuse and the medial temporal lobe structures were most affected (15-24% reduction) followed by the inferior parietal, precuneus and posterior cingulate (5-10% reduction). In DLB, the average cortical thinning in the medial temporal lobe structures was less (6-10% reduction) than for AD and similar to the reduction in cortical thickness observed in other

regions. The percentage reduction in CTh in the inferior parietal, precuneus and posterior cingulate (5-9%) were similar to that observed in AD. In DLB, the transverse temporal gyri and right precentral gyri were areas that had more cortical thinning compared with healthy subjects than observed in AD.

Cortical thickness and cognitive and clinical measures

In DLB subjects there was a positive association between MMSE and CTh in the left superior frontal, superior temporal and parahippocampal gyri and right posterior cingulate, insula and fusiform gyri (Figure 2 (a); $n=31$, $df=27$, $t>2.8$, $p<0.01$ uncorrected). We did not find an association between MMSE and CTh in AD ($n=30$, $df=26$, $t<2.1$, $p>0.05$ uncorrected). Performance on letter fluency also positively correlated with CTh in the left precuneus, precentral, superior frontal (anterior cingulate), lingual and postcentral gyri and right fusiform, precuneus, lateral orbitofrontal and inferior parietal in DLB ($n=31$, $df=27$, $t>2.8$, $p<0.01$ uncorrected). These associations are represented in Figure 2 (b). We did not find an association between cortical thickness and letter fluency performance in AD ($n=30$, $df=26$, $t<2.1$, $p>0.05$ uncorrected).

DISCUSSION

Patterns of cortical thinning differed in DLB and AD when compared to a group of similarly aged older subjects. AD was characterised by cortical thinning in the medial temporal and temporo-parietal association cortices as well as areas of the frontal cortices. DLB was characterised by more localised areas of cortical thinning predominantly affecting the posterior parietal cortices with relative sparing of the frontal and medial

temporal structures. Correlations between MMSE and verbal fluency and CTh in DLB were also observed in key cortical regions.

In DLB, there was localised cortical thinning in the posterior parietal association cortices. Functional imaging studies using SPECT have reported precuneal and occipital hypoperfusion.(19, 20) However, structural imaging studies have not consistently reported change.(21, 22) We have previously reported the results of structural change in this cohort using VBM analysis and visual rating scales.(7, 23) Whilst there was a pattern suggestive of posterior atrophy using VBM, it did not reach statistical significance when corrected for multiple comparisons (high probability of false positives) and using a visual rating scale there was no significant difference when compared to either healthy individuals or AD.(7, 23) By contrast, a pattern of highly significant white matter tract change in the parieto-occipital areas was observed using diffusion tensor imaging.(24) Cortical thinning in DLB may be a result of secondary grey matter loss following white matter tract degeneration, or vice versa. Further studies using multimodal analysis techniques and longitudinal assessment may help to address this. It may also be that measurements of cortical thickness are a more sensitive means for studying regional patterns of grey matter atrophy. The inferior longitudinal fasciculus connects the occipital lobe to the temporal pole and runs in the inferior temporal gyri, hypothesised to form the ventral visual stream, with the temporal pole also receiving input from the anterior cingulate via the uncinate fasciculus. We observed focal areas of cortical thinning in the temporal pole and lateral temporal structures, areas that have also been reported to be associated with Lewy related pathology and visual hallucinations.(25) We

also found cortical thinning in the posterior cingulate with the average loss similar to Alzheimer's disease. The posterior cingulate forms the central node of the default mode network and receives input from the thalamus, an important structure for attentional function with projections to the precuneus. The posterior cingulate in DLB has also been found to be vulnerable to amyloid deposition using PET with amyloid burden being associated with visuo-spatial dysfunction.(26) Our findings of cortical thinning in this region highlight the posterior cingulate as an area of vulnerability and importance in the pathogenesis of DLB.

The medial temporal structures were profoundly affected in AD. In particular the entorhinal cortex and parahippocampal gyri had the most extensive cortical loss. As expected, there was much less cortical thinning observed in these regions in DLB which is consistent with other imaging (7, 22) and pathological studies (27, 28) as well as the relative sparing (when compared to AD) of episodic memory observed.(29) Interestingly, the average percentage cortical loss in the medial temporal structures in DLB was similar to other (lateral) temporal and parietal regions. Whilst, it is possible that the medial temporal atrophy observed may be due to Alzheimer pathology, the differential gradient suggests that other pathophysiological mechanisms may be contributing.

We found a positive association between cortical thickness measures in temporal structures including fusiform, insula and superior temporal gyrus, the right posterior cingulate and left superior frontal and MMSE. Therefore, in DLB subjects, cortical thinning in these regions appeared to be associated with greater disease severity as

measured by the MMSE. Although these results need to be interpreted with the important caveat that they are reported uncorrected for multiple comparisons (increased Type I error). This association was not observed in AD, which may, in part be due to floor effects as in AD many of these structures are affected early and more profoundly. Given the groups were of similar level of dementia severity, it suggests that there are differing pathophysiological mechanisms underpinning the global cognitive changes in DLB and AD.

We also found a positive association between letter fluency and CTh in the frontal and parietal structures in DLB and not AD. This indicates that subjects with greater cortical thinning in these regions were more likely to perform poorly on the letter fluency task. Generally patients with DLB are characterised by a dysexecutive syndrome with the fronto-striatal network being implicated (29). However, functional imaging studies indicate that input from the temporal and parietal association cortices are also required (30). The precuneus is an important and potentially vulnerable structure in DLB as demonstrated in functional imaging studies (19). The association between CTh in this region and more impaired verbal fluency suggests its clinical importance in the pathogenesis of DLB and how it differs to AD.

Cortical thickness measurement using MRI may be a more sensitive measure of structural grey matter change. It offers novel insights into important structural imaging differences between the conditions. Interestingly, a recent logistic regression study of pathologically confirmed cases using selected regions on antemortem structural MRI found excellent

diagnostic sensitivity in DLB, highlighting the potential for structural MRI measures as a useful biomarker in distinguishing between the conditions.(31) Others have also reported excellent diagnostic sensitivity in DLB when combining multi-modal imaging variables from PiB-PET, FDG-PET and structural MRI in DLB and AD.(32) At this stage, the clinical and treatment implications of cortical thickness measurement are somewhat limited and further studies are required to address the potential diagnostic utility. Furthermore, the analysis procedures involved in the technique also currently limit its clinical utility. However, improved computational systems and machine learning techniques using computer based classification methods would assist the development of this as a clinically useful investigation and warrants further investigation and development.

Strengths of the study include a well-characterised group of probable DLB and AD patients. In addition, the healthy comparison group were well matched for age and educational level. Subject groups were based on clinical rather than pathological confirmation, a limitation of all ante-mortem imaging studies. In addition, it is likely that a proportion of healthy subjects will also have preclinical disease which would potentially reduce the reported difference. During the FreeSurfer processing we had an 11% failure rate, similar to other groups. The inclusion of 2 T1 weighted scans has been suggested to improve this and may be a consideration for future work.

Cortical thickness may be a sensitive measure for characterising grey matter atrophy in DLB and highlights the structural imaging differences between the conditions. It may have a valuable role in distinguishing groups, although requires further investigation.

	Healthy subjects	DLB	AD	p value
<i>n</i>	33	31	30	
Gender (m: f)	19: 14	26: 5	16: 14	$\chi^2=7.4, 0.02$
Age (year)	76.8 ± 5.3	77.8 ± 7.1	77.9 ± 5.7	$F_{2,91}=0.35, p=0.71$
MMSE	29.0 ± 1.0	20.6 ± 5.1	19.5 ± 4.7	$H_2=59.9, p<0.001^\dagger$
CAMCOG	97.0 ± 3.7	68.3 ± 15.1	65.5 ± 11.4	$H_2=60.0, p<0.001^{\dagger\dagger}$
UPDRS III	2.0 ± 1.9	26.0 ± 10.3	5.6 ± 4.5	$H_2=65.7, p<0.001^{\dagger\dagger\dagger}$

Table 1. Demographic and group characteristics.

Values expressed as Mean ± 1SD.

Post Hoc Mann-Whitney U tests:

[†]HS > AD ($U_{63}=47.9, p<0.001$), HS > DLB ($U_{64}=42.6, p<0.001$), AD vs. DLB ($U_{61}=5.3, p=1.0$).

^{††} HS > AD ($U_{63}=50.0, p<0.001$), HS > DLB ($U_{64}=43.0, p<0.001$), AD vs. DLB ($U_{61}=4.9, p=1.0$).

^{†††} HS > AD ($U_{63}=17.0, p=0.04$), HS > DLB ($U_{64}=54.1, p<0.001$), AD vs. DLB ($U_{61}=37.1, p<0.001$).

Abbreviations: DLB, dementia with Lewy bodies; AD, Alzheimer's disease; HS, Healthy subjects; MMSE, Mini-Mental State examination; CAMCOG, Cambridge Cognitive Examination; UPDRS III, Unified Parkinson's Disease Rating Scale, Part III.

	BA	x	y	z	Vtx	Area	$-\log_{10}P$
(a) Healthy subjects vs. DLB							
Left medial orbitofrontal	11	-8	30	-16	206	133	3.77
Left superior frontal	8	-7	26	44	235	142	3.75
Left superior temporal	22	-51	-6	-7	1353	751	4.09
Left inferior temporal	36	-48	-41	-22	1018	636	5.21
Left temporal pole	38	-35	13	-34	418	235	3.91
Left fusiform	37	-34	-43	-9	503	229	4.36
Left superior parietal	7	-31	-56	60	1055	434	4.46
Left inferior parietal	19	-38	-82	26	7594	4135	6.50
Left posterior cingulate	7	-7	-33	41	1052	444	5.68
Right superior frontal	9	9	31	34	467	245	4.47
Right superior temporal	38	43	11	-26	3813	2024	6.49
Right middle temporal	21	56	-57	7.1	835	425	5.09
Right fusiform	37	37	-43	-11	1790	882	6.84
Right precuneus	19	20	-78	36	1085	678	4.38
Right superior parietal	7	13	-65	60	106	45	3.68
Right inferior parietal	40	55	-52	35	510	255	4.04
Right posterior cingulate	24	5	-22	39	509	221	4.23
(b) Healthy subjects vs. AD							
Left medial orbitofrontal	11	-8	25	-14	903	486	3.90
Left superior frontal	32	-20	19	57	4666	2771	3.62
Left paracentral	5	-5	-42	65	525	228	3.11
Left entorhinal	35	-20	-14	-27	53805	26764	11.88
Right superior frontal	6	10	28	35	2159	1140	5.12
Right entorhinal	28	21	-13	-27	54043	27651	9.18

Table 2. Location and peak vertex significance of cortical thinning in DLB (two-sample t-test, $df=60$) and AD (two-sample t-test, $df=59$) compared to healthy older subjects. For each peak, table shows anatomical region, Brodmann area, Talairach coordinates, Number of vertices (Vtx), Surface area (Area) (mm^2), vertex-level significance ($P_{\text{FDR-Corr}}$). All results are significant $p < 0.005$, False Discovery Rate (FDR) corrected (e.g., $-\log_{10}P = 3$ corresponds to $p=0.001\dots$ etc). BA=Brodmann area, Vtx=Number of Vertices, Area=surface Area.

	AD	DLB	AD CTh %	DLB CTh %
Left precentral gyrus	2.24 ± 0.28	2.26 ± 0.19	6.0	4.9
Left entorhinal cortex	2.38 ± 0.42	2.89 ± 0.45	23.4	7.3
Left parahippocampal gyrus	2.10 ± 0.25	2.32 ± 0.35	15.5	6.7
Left transverse temporal	2.19 ± 0.24	2.07 ± 0.29	3.6	8.6
Left inferior parietal	2.22 ± 0.13	2.28 ± 0.22	10.5	8.3
Left precuneus	2.16 ± 0.19	2.23 ± 0.17	8.3	5.5
Left posterior cingulate	2.33 ± 0.26	2.30 ± 0.17	5.3	6.6
Right precentral gyrus	2.28 ± 0.23	2.21 ± 0.20	3.8	6.8
Right entorhinal cortex	2.43 ± 0.53	2.87 ± 0.49	23.6	9.7
Right parahippocampal gyrus	2.09 ± 0.35	2.29 ± 0.27	16.4	8.3
Right transverse temporal	2.25 ± 0.28	2.13 ± 0.24	2.0	7.3
Right inferior parietal	2.25 ± 0.22	2.26 ± 0.18	7.8	7.6
Right posterior cingulate	2.26 ± 0.23	2.27 ± 0.15	5.2	4.8

Table 3. Cortical thickness (CTh) in selected brain regions in AD and DLB. Average cortical thickness derived from the Desikan template is expressed in mm (Mean ± 1 SD). CTh% = difference in the average cortical thickness (in AD and DLB) compared to the healthy comparison group, expressed as a percentage reduction.

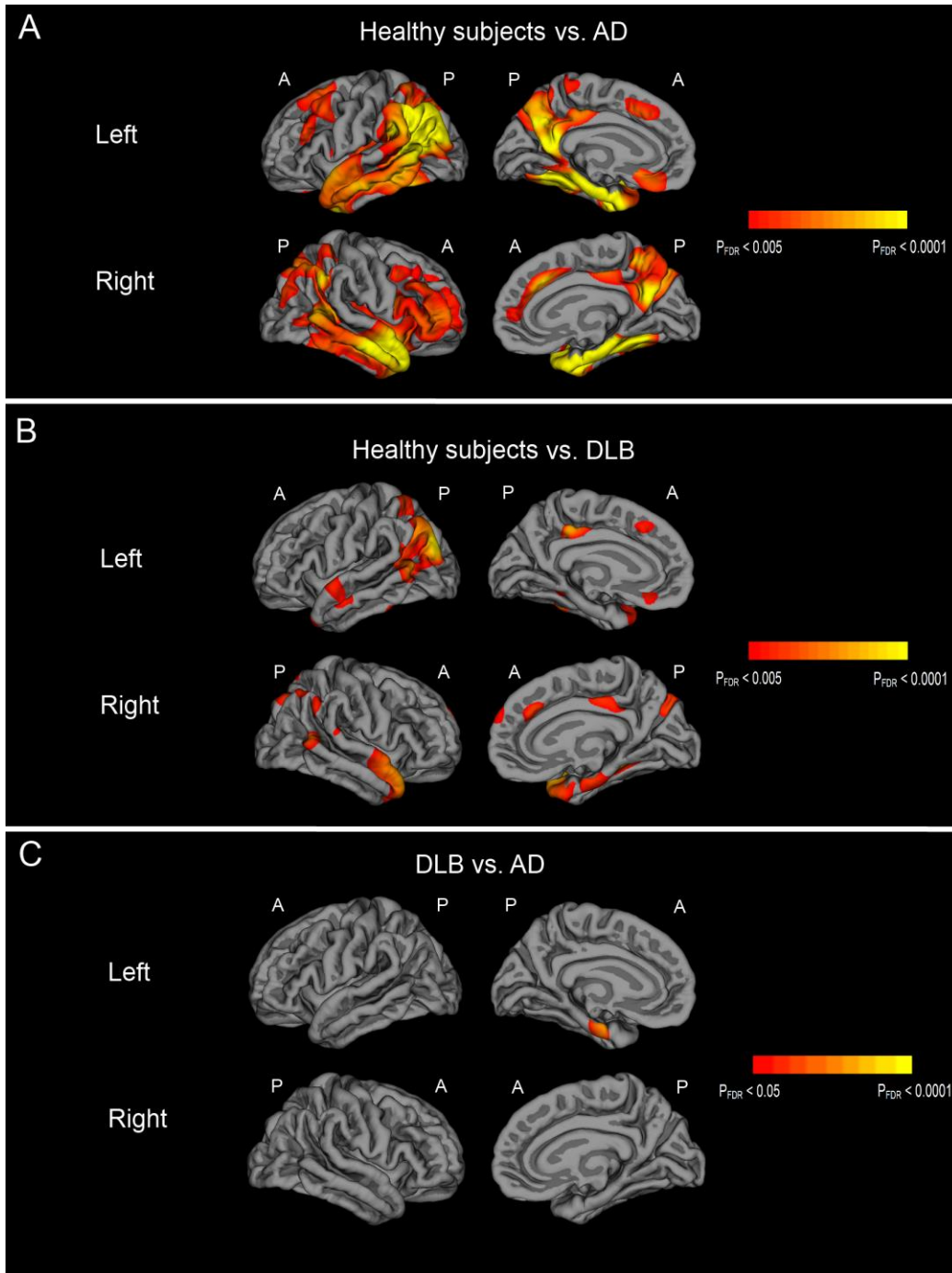


Figure 1. Patterns of cortical thinning across groups. Significantly thinner cortex in patients with (A) Alzheimer’s disease compared to healthy older individuals (two-sample t-test, $df=59$), (B) dementia with Lewy bodies compared to healthy older individuals (two-sample t-test, $df=60$) and (C) Alzheimer’s disease compared to dementia with Lewy bodies (two-sample t-test, $df=57$). Areas of significant cortical thinning are represented in red/orange/yellow as indicated by the coloured bar (False Discovery Rate corrected p values).

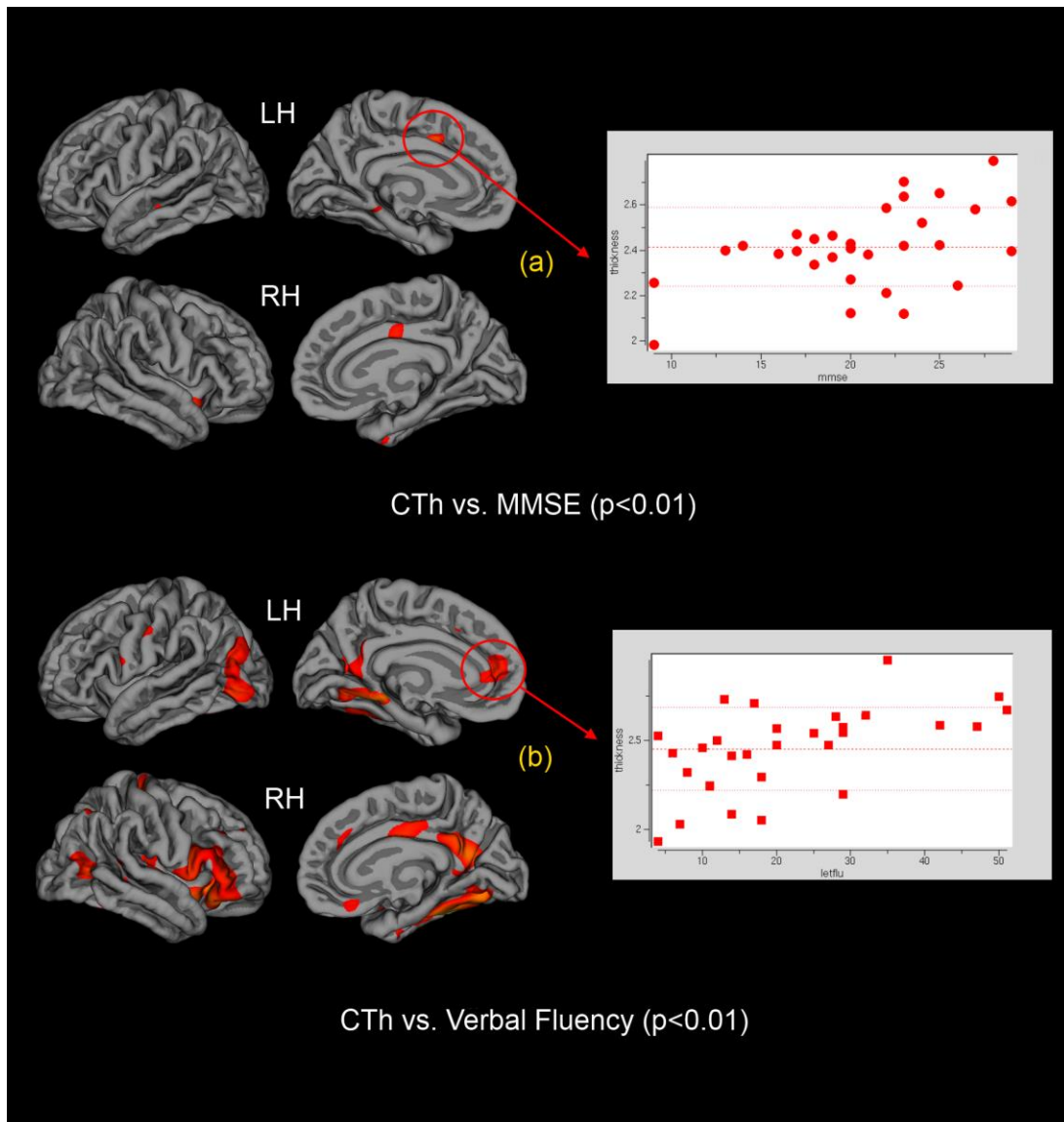


Figure 2. Correlation between cortical thickness (CTh) and clinical features in DLB. Relationship between CTh and MMSE score (a) and Verbal (letter) Fluency (b) (linear regressions, $df=27$). Graphical representation of the CTh measurement and clinical variable in selected regions are also displayed. LH, left hemisphere; RH, right hemisphere; CTh, cortical thickness; MMSE, mini-mental state examination. Results shown are uncorrected p values.

References

1. Voets NL, Hough MG, Douaud G, et al: Evidence for abnormalities of cortical development in adolescent-onset schizophrenia. *Neuroimage* 2008; 43:665-675
2. Winkler AM, Kochunov P, Blangero J, et al: Cortical thickness or grey matter volume? The importance of selecting the phenotype for imaging genetics studies. *Neuroimage* 2010; 53:1135-1146
3. Du AT, Schuff N, Kramer JH, et al: Different regional patterns of cortical thinning in Alzheimer's disease and frontotemporal dementia. *Brain* 2007; 130:1159-1166
4. Lehmann M, Crutch SJ, Ridgway GR, et al: Cortical thickness and voxel-based morphometry in posterior cortical atrophy and typical Alzheimer's disease. *Neurobiol Aging* 2011; 32:1466-1476
5. McKhann G, Drachman D, Folstein M, et al: Clinical diagnosis of Alzheimer's disease: report of the NINCDS-ADRDA Work Group under the auspices of Department of Health and Human Services Task Force on Alzheimer's Disease. *Neurology* 1984; 34:939-944
6. McKeith IG, Dickson DW, Lowe J, et al: Diagnosis and management of dementia with Lewy bodies: third report of the DLB Consortium. *Neurology* 2005; 65:1863-1872
7. Watson R, O'Brien JT, Barber R, et al: Patterns of gray matter atrophy in dementia with Lewy bodies: a voxel-based morphometry study. *Int. Psychogeriatr.* 2012; 24:532-540
8. Folstein M, Folstein S, McHugh P: "Mini-mental state". A practical method for grading the cognitive state of patients for the clinician. *Journal of Psychiatric Research.* 1975; 12:189-198
9. Fahn S, Elton R, Committee amotUD: Unified Parkinson's Disease Rating Scale, in *Recent development in Parkinson's Disease*. Edited by Fahn S, Marsden C, Calne D, et al. Florham Park, Macmillan Health Care Information, 1987, pp 153-164
10. Cummings JL, Mega M, Gray K, et al: The Neuropsychiatric Inventory: comprehensive assessment of psychopathology in dementia. *Neurology* 1994; 44:2308-2314
11. Bucks RS, Ashworth DL, Wilcock GK, et al: Assessment of activities of daily living in dementia: development of the Bristol Activities of Daily Living Scale. *Age and Ageing* 1996; 25:113-120
12. Dale AM, Fischl B, Sereno MI: Cortical surface-based analysis. I. Segmentation and surface reconstruction. *Neuroimage* 1999; 9:179-194
13. Fischl B, Dale AM: Measuring the thickness of the human cerebral cortex from magnetic resonance images. *Proc Natl Acad Sci U S A* 2000; 97:11050-11055
14. Fischl B, Sereno MI, Dale AM: Cortical surface-based analysis. II: Inflation, flattening, and a surface-based coordinate system. *Neuroimage* 1999; 9:195-207
15. Desikan RS, Segonne F, Fischl B, et al: An automated labeling system for subdividing the human cerebral cortex on MRI scans into gyral based regions of interest. *NeuroImage* 2006; 31:968-980
16. Fischl B, van der Kouwe A, Destrieux C, et al: Automatically parcellating the human cerebral cortex. *Cerebral cortex (New York, N.Y. : 1991)* 2004; 14:11-22
17. Ashburner J, Friston KJ: Unified segmentation. *NeuroImage* 2005; 26:839-851

18. Genovese CR, Lazar NA, Nichols T: Thresholding of statistical maps in functional neuroimaging using the false discovery rate. *Neuroimage* 2002; 15:870-878
19. Colloby SJ, Fenwick JD, Williams ED, et al: A comparison of Tc-99m-HMPAO SPET changes in dementia with Lewy bodies and Alzheimer's disease using statistical parametric mapping. *European Journal of Nuclear Medicine and Molecular Imaging* 2002; 29:615-622
20. Lobotesis K, Fenwick JD, Phipps A, et al: Occipital hypoperfusion on SPECT in dementia with Lewy bodies but not AD. *Neurology* 2001; 56:643-649
21. Middelkoop HA, van der Flier WM, Burton EJ, et al: Dementia with Lewy bodies and AD are not associated with occipital lobe atrophy on MRI. *Neurology* 2001; 57:2117-2120
22. Whitwell JL, Weigand SD, Shiung MM, et al: Focal atrophy in dementia with Lewy bodies on MRI: a distinct pattern from Alzheimer's disease. *Brain* 2007; 130:708-719
23. O'Donovan J, Watson R, Colloby SJ, et al: Does posterior cortical atrophy on MRI discriminate between Alzheimer's disease, dementia with Lewy bodies, and normal aging? *International psychogeriatrics / IPA* 2012; 1-9
24. Watson R, Blamire AM, Colloby SJ, et al: Characterizing dementia with Lewy bodies by means of diffusion tensor imaging. *Neurology* 2012; 79:906-914
25. Harding AJ, Broe GA, Halliday GM: Visual hallucinations in Lewy body disease relate to Lewy bodies in the temporal lobe. *Brain* 2002; 125:391-403
26. Gomperts SN, Rentz DM, Moran E, et al: Imaging amyloid deposition in Lewy body diseases. *Neurology* 2008; 71:903-910
27. Burton EJ, Barber R, Mukaetova-Ladinska EB, et al: Medial temporal lobe atrophy on MRI differentiates Alzheimer's disease from dementia with Lewy bodies and vascular cognitive impairment: a prospective study with pathological verification of diagnosis. *Brain* 2009; 132:195-203
28. Kantarci K, Ferman TJ, Boeve BF, et al: Focal atrophy on MRI and neuropathologic classification of dementia with Lewy bodies. *Neurology* 2012; 79:553-560
29. Metzler-Baddeley C: A review of cognitive impairments in dementia with Lewy bodies relative to Alzheimer's disease and Parkinson's disease with dementia. *Cortex* 2007; 43:583-600
30. Collette F, Hogge M, Salmon E, et al: Exploration of the neural substrates of executive functioning by functional neuroimaging. *Neuroscience* 2006; 139:209-221
31. Vemuri P, Simon G, Kantarci K, et al: Antemortem differential diagnosis of dementia pathology using structural MRI: Differential-STAND. *NeuroImage* 2011; 55:522-531
32. Kantarci K, Lowe VJ, Boeve BF, et al: Multimodality imaging characteristics of dementia with Lewy bodies. *Neurobiol Aging* 2012; 33:2091-2105